Journal of Alloys and Compounds 505 (2010) 467–471

Contents lists available at ScienceDirect

Journal of Alloys and Compounds

journal homepage: www.elsevier.com/locate/jallcom

The influence of structure on thermal behavior of reactive Al–Ni powder mixtures formed by ball milling

A. Hadjiafxenti[a], I.E. Gunduz[a,*], C. Tsotsos[a], T. Kyratsi[a], S.M. Aouadi[b], C.C. Doumanidis[a], C. Rebholz[a,c]

[a] Mechanical and Manufacturing Engineering Department, University of Cyprus, 1678 Nicosia, Cyprus
[b] Department of Physics, Southern Illinois University Carbondale, Carbondale, IL 62901-4401, USA
[c] Mechanical and Industrial Engineering Department, Northeastern University, Boston, MA 02115, USA

ARTICLE INFO

Article history:
Received 18 February 2010
Received in revised form 22 March 2010
Accepted 31 March 2010
Available online 19 June 2010

Keywords:
Mechanical alloying
Intermetallics
Metals and alloys
Nanostructured materials
Diffusion
Self-propagating reactions

ABSTRACT

Ball milling (BM) was used to produce reactive Al–Ni powder mixtures that exhibit self-propagating exothermic reactions (SPER) for nano–micro heater applications. Powders with an Al–Ni molar ratio of 1:3 were milled, cold pressed into pellets and ignited using a heat source. The structural and thermal properties of the pellets were characterized before and after ignition using X-ray diffraction (XRD), scanning electron microscopy (SEM) and differential scanning calorimetry (DSC). The reaction characteristics of the pellets were evaluated using an infrared camera during ignition experiments. Pellet microstructures show that the BM technique created nanoscale lamellar structures, with dimensions diminishing with increasing milling time. Pellets milled longer than 16 h exhibited SPER. Flame velocity increased with pellet density.

1. Introduction

In recent years, there has been considerable effort in investigating various material systems for micro/nanoscale device manufacturing through thermal material removal, deposition, joining, or shaping. However, there are fundamental technical limits that prohibit the use of traditional heat sources for such miniaturized systems [1]. Methods taking advantage of the energy released by nanoscale materials that exhibit self-propagating exothermic reactions (SPER) are a promising alternative for thermal manufacturing owing to their ability to provide intense localized heat. Alternating nanoscale layers of selected materials that exhibit exothermic reactions produced in thin film form using vacuum deposition methods require expensive equipment and long processing times [2–5]. A potential economical method to produce nanoscale lamellar structures that exhibit SPER is ball milling (BM) [6–9]. BM is a simple technique that provides mechanical energy to the powders through repeated collision events with steel or ceramic balls in a rotating drum. Milling parameters, such as ball mass and material, ball to powder weight ratio, rotation velocity and duration influence the resulting microstructure of the pellets. Continuous micro-welding and shearing of the powders facilitate the formation of nanoscale microstructures and intermetallic or amorphous phases [10]. The microstructure of the pellets, in turn, is expected to influence their ignition and reaction characteristics.

In this study, we selected the Al–Ni system to be investigated because both powders are relatively inexpensive, and their reactions are highly exothermic and well characterized [11–14]. A low-energy ball miller was used to process these powders without forming nickel aluminides. The compacted powders were ignited thermally to initiate the exothermic reactions. The temperature of the pellets was monitored using an infrared (IR) camera and the reaction speed was correlated to the ball milling parameters, ignition processing conditions and compact density.

2. Experimental

A low-energy Fritsch Planetary Mono Mill "Pulverisette 6" was used for milling Al and Ni powders in nitrogen atmosphere. The mesh size of the powders was 325, the molar ratio was 1:3, corresponding to the molar ratio of $AlNi_3$ intermetallic compound, and the purity was 99.5% and 99.95%, respectively. The total weight of the powders was 32 g. Milling was performed in an 80 ml vial with a rounded cylindrical volume, using five 20 mm diameter stainless steel balls. The starting ball to powder weight ratio was 5.1:1 and the rotational speed of the miller was set to 300 rpm.

The BM run was interrupted every 2 h, with the first interval at 4 h and the last one at 22 h. During each interval, 2 g of the sample material was removed for analysis and ignition experiments. In order to avoid exposure to air, the sample removal procedure was conducted in a nitrogen filled glove box.

Pellets, 10 mm in diameter and 1.3 mm in thickness, were formed by pressing 0.5 g of the powder under a pressure of 50.9 MPa. The pellets were analyzed before

* Corresponding author. Tel.: +357 99927618.
E-mail address: emreth@ucy.ac.cy (I.E. Gunduz).

0925-8388/$ – see front matter © 2010 Elsevier B.V. All rights reserved.
doi:10.1016/j.jallcom.2010.03.250

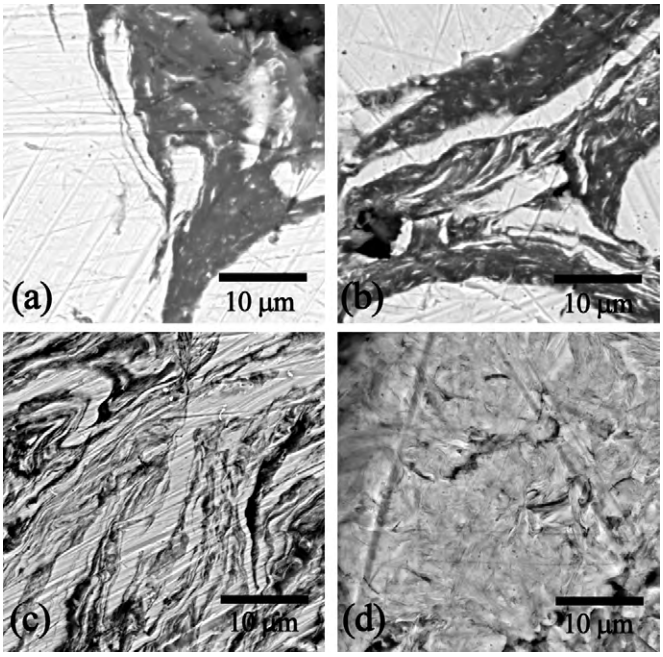

Fig. 1. SEM images of the (a) 6 h, (b) 12 h, (c) 18 h and (d) 22 h polished samples.

and after ignition experiments, using scanning electron microscopy (SEM – Tescan Vega LSU) and X-ray diffraction (XRD – Shimadzu 6000 Series). Differential scanning calorimetry (DSC – Linseis TG-DTA/DSC) measurements were carried out at a heating rate of 10 K/min with temperatures up to 1773 K.

The pellets were ignited in air using a propane torch (flame temperature ~2200 K) with its nozzle 30 mm away from the sample. The flame from the torch covered only the edge of the pellet and was removed when ignition was established, which is characterized by a rapid increase in temperatures outside the flame affected area. The ignition time is defined as the time it takes for the reaction to start. The ignition process was recorded using a FLIR System A40 Thermovision IR camera operated at 50 frames/s with a temperature range of 573–1973 K to measure (a) the ignition temperature (IT), which is the recorded temperature in the heated zone under the flame when the reaction begins, (b) the sample temperature (ST), which is the average temperature of the rest of the sample at the time of ignition and (c) the pellet overall maximum temperature (MT) reached as the reaction progresses, which was nearly constant along the pellet surface for all samples. The hemispherical emissivity of the pellets was measured before and after reaction using a hot plate and the IR camera for calibration.

A separate batch of 7.5 g of Al–Ni powders with a 1:3 molar ratio was milled for 4 h and consolidated at 12.7, 25.5, 38.2, 50.9 and 63.6 MPa with thicknesses 1.7, 1.5, 1.4, 1.3 and 1.25 mm, correspondingly, and ignited to investigate the effect of pellet density and porosity on flame front velocity.

3. Results and discussion

The microstructure of samples ball-milled for 6, 12, 18 and 22 h is shown in Fig. 1. Longer milling durations result in finer microstructural features. After 6 h, softer Al particles mechanically mix with micro-welded Ni fragments and accommodate most of the plastic deformation, whereas hard Ni particles do not experience significant deformation (Fig. 1(a)). Fragmentation of the Ni particles increases after 12 h of milling accompanied by more boundary welding and shear deformation, and lamellar morphology starts to emerge (Fig. 1(b)). This is due to the hardening of the Al-rich matrix, resulting in more efficient load transfer to the Ni particles. Further milling (18 h) results in the formation of a finer lamellar structure as the mechanical and thermal shocks generate aggregates [8,15] composed of thin layers of Al and Ni along with the remaining larger highly deformed Ni particles (Fig. 1(c)). Similar observations are made for samples processed for 22 h. However, much finer lamellar structures are observed and no Ni particle remains at this stage (Fig. 1(d)).

The XRD patterns of the 6, 12, 18 and 22 h specimens before and after ignition tests are shown in Fig. 2. Only symmetric Al and Ni peaks are discernible in the as-milled samples except for the 22 h sample, which shows asymmetric overlapping peaks. It has been speculated that ball-milled powders equivalent to the 22 h samples in this study, show the formation of a single phase $AlNi_3$ with the absence of superlattice peaks, which is then attributed to this phase being disordered [16]. However, this final product might instead be a very fine mixture with compositions ranging from extended Ni-rich solid-solutions and $AlNi_3$ to AlNi with broad overlapping peaks, because Fig. 1(d) clearly shows some compositional variation within the particles.

Ignition results in the formation of AlNi and $AlNi_3$ intermetallic compounds (Fig. 2). The relative peak intensities of the intermetallics vary with milling time, proportional to their present quantities. For example, the ignited 12 h sample consists of mostly AlNi and some $AlNi_3$, whereas for the ignited 18 h sample, $AlNi_3$ is the major phase that is present. In the Al–Ni system, AlNi phase has

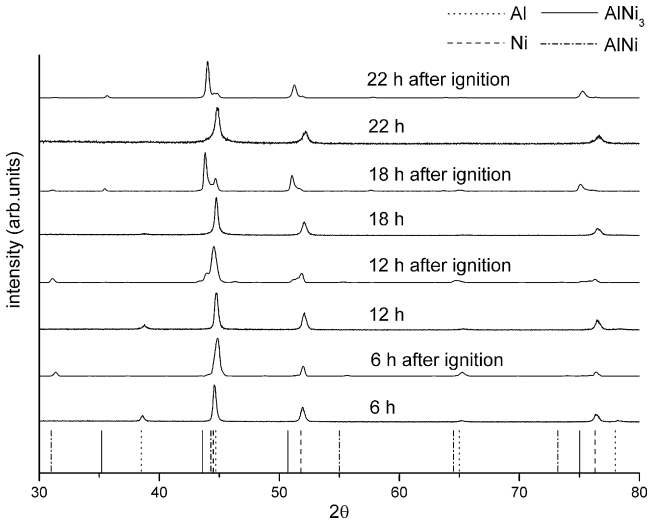

Fig. 2. XRD patterns of the 6, 12, 18 and 22 h samples before and after ignition tests.

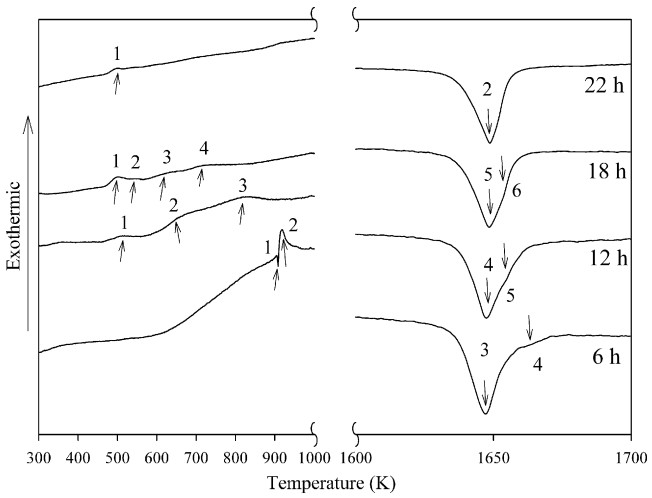

Fig. 3. DSC traces of the 6, 12, 18 and 22 h samples.

the highest formation enthalpy and its formation is thermodynamically favored. Therefore, it is most probable that AlNi is always the first phase to form rapidly during reactions, but some of it transforms into $AlNi_3$ at the layer interfaces through enhanced diffusion (due to the existence of many nanoscale layers compared to bulk) when temperatures rise locally. For lower milling times, the local composition within lamella are closer to AlNi composition as some of the Ni remains separate (Fig. 1(b)), which would reduce the formation of $AlNi_3$. With increasing milling time, more of the Ni is incorporated into the lamellae through mixing (Fig. 1(c)), increasing the local compositions closer to $AlNi_3$, resulting in increased amounts of this phase. None of the other intermetallic phases are stable at the reaction temperatures involved, hence their peaks are absent in the spectra. Ni peaks remain in all of the ignited samples, so the phase transformation is never complete after the reactions. This is due to the relatively large dimensions of the remaining Ni layers shown in Fig. 1 for different milling times.

DSC traces show that increasing milling time results in additional peaks as well as a general peak shifting trend towards lower temperatures, related to further mixing and lamellae refinement (Fig. 3), similar to those observed in continuously rolled Al and Ni multilayer foils [17]. The 6 h sample shows four peaks at (1) 905 K (endothermic), (2) 910 K (exothermic), (3) 1630 K (endothermic) and (4) 1660 K (endothermic). The 12 h milled sample exhibits three exothermic peaks centered at (1) 513 K, (2) 660 K, (3) 827 K. Additionally, there are two endothermic peaks at (4) 1630 K and (5) 1650 K. The 18 h milled sample shows four exothermic peaks centered at (1) 506 K, (2) 550 K, (3) 639 K and (4) 723 K and similar endothermic peaks at (5) 1630 K and (6) 1650 K. The comparison of the results with other work suggests the formation of nanoscale structures within 18 h of milling [4,7,18,19]. The low temperature peaks are most probably associated with the formation of Al_9Ni_2, Al_3Ni and $AlNi_3$, similar to those observed in nanoscale multilayer foils with a bilayer thickness of 200 nm [4]. The 22 h milled sample shows one exothermic peak centered around (1) 500 K and an endothermic peak starting around (2) 1630 K. Contrary to shorter durations, there are no other peaks in between and at ~1650 K. Furthermore, the total amount of heat released is less than that measured for other samples, possibly due to the formation of some intermetallic phases during milling. The 1630 and 1650 K peaks probably correspond to the melting of $AlNi_3$ and Ni as there are no other possible endothermic reactions at these temperatures in the Al–Ni system.

Table 1 shows the ignition characteristics of the samples as a function of milling time. In general, increasing the milling time

Table 1
Ignition test temperature measurements as a function of ball milling time.

BM time (h)	IT (K)	ST (K)	MT (K)
6	1414	1414	>1973
8	1251	1251	>1973
10	1453	1453	>1973
12	1126	952	>1973
14	1289	797	>1973
16	873	581	>1973
18	821	<573	1644
20	904	<573	1580
22	891	<573	1375

resulted in substantial decrease in the required ignition time due to smaller diffusion distances across the more refined lamellar structures [20–24]. Furthermore, the results suggest that the pellets may be grouped into two categories. The first category includes samples milled for up to 14 h, characterized by an ignition temperature (IT) between 1126 and 1455 K. In this case, complete reaction was only observed after sample temperature (ST) reached values in the vicinity of IT. The recorded maximum temperature (MT) was near the maximum calibration limit of the IR camera (1973 K). The second group of samples consist of pellets ball-milled for more than 14 h. These samples exhibited SPER relatively fast without requiring a substantial increase in ST with IT values near the melting temperature of Al (~933 K).

Fig. 4(a) and (b) show the difference between the reaction modes among the samples milled for 12 and 18 h, respectively, where the temperature profiles are obtained along the diameter of the pellets. Heating of the 12 h sample initiated complete reaction only after the temperature of the entire pellet (ST) increased above 950 K. The flame front uniformly affected the whole sample, and after removing the heat source ($t = 0$ s), the temperature increased until $t = 1.24$ s to the maximum recorded temperature (MT) (Fig. 4(a)). In contrast, the flame front of the 18 h sample appeared sharper where the front started at the heated edge and travelled rapidly across the pellet, also evident in the measured temperature profiles (Fig. 4(b)). The MT values for samples milled for up to 16 h are significantly higher than the room temperature adiabatic formation temperature of $AlNi_3$ (~1600 K [25]), as these samples require extensive heating until reaction was initiated (thus higher ST during ignition).

Two different propagation modes were suggested by Moore and Feng [26] and are referred to as simultaneous combustion mode versus self-propagating mode. In the first mode, overall sample temperature is required to be kept high, as was the case for the 12 h sample. This mode is observed for microscale sputtered multilayers and powder mixtures where the large diffusion distances prohibit a sustained reaction in the presence of high thermal gradients ahead of the flame front due to cooling [25]. In the second mode, the flame front is able to self-propagate in spite of the cooling effect, due to shorter diffusion distances across adjacent layers and faster intermetallic growth. This phenomenon was observed in the 18 h sample as well as in sputtered nanoscale multilayers [2,4,5].

The MT values decreased as milling times increased from 18 to 22 h. MT for the 18 h sample is near the room temperature adiabatic formation temperature of $AlNi_3$ (~1600 K [26]), indicating optimum reaction conditions. It is possible that some intermetallics have started to form at the lamellae interfaces during further milling [9,15], which would decrease the available excess enthalpy and produce lower MT values. This is also suggested by the propagation velocities of 18, 20 and 22 h samples, which were 0.38, 0.25 and 0.1 m/s, respectively. For sputtered nanoscale multilayer foils, low temperature annealing was shown to generate intermetallics at the interfaces and result in lower flame velocities, as these phases act as diffusion barriers [5].

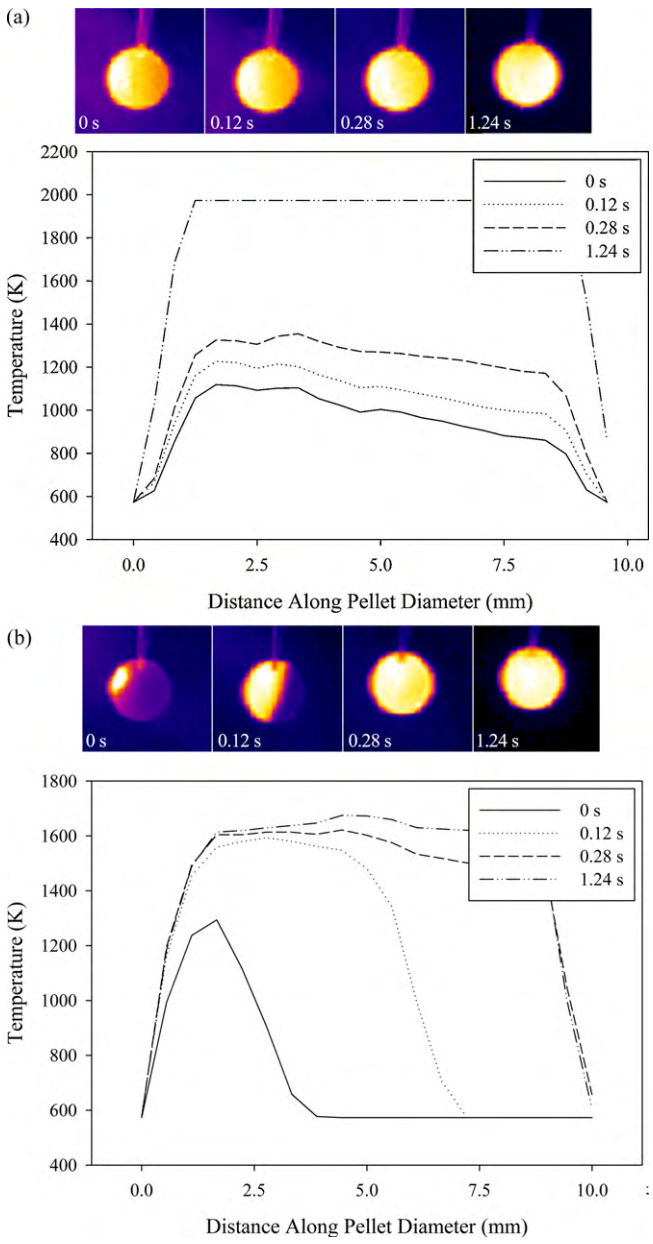

Fig. 4. Infrared camera images of the reaction and the temporal evolution of temperature profiles of the surface of the pellets along the diameter for (a) 12 h and (b) 18 h milled samples at ignition (0 s) and after 0.12, 0.28 and 1.24 s.

The flame front velocities measured for the second set of BM (4 h milling time and a total mass of 7.5 g) was found to increase with pellet density, as shown in Fig. 5. This is due to better thermal contact between particles compacted at higher pressures resulting in lower porosity (higher densities) [27]. The best fit was a weak exponential function, slightly better than a second order polynomial. The non-linear nature of the curve suggests this effect not only directly increases the rate of heat transfer due to reduced thermal resistance between particles, but also the diffusive mass transfer across particles due to the breaking-up of surface oxides, hence the deviation from a linear behavior. There was no dependence of the maximum temperatures reached (1973 ± 25 K) on the measured densities, suggesting that reaction heats are not affected and the effect is only kinetic.

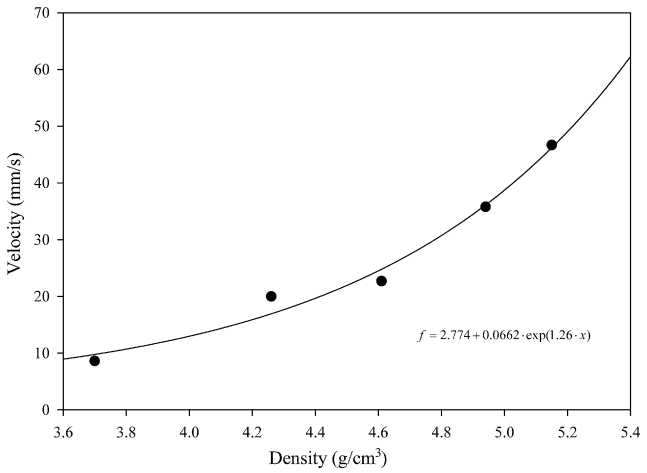

Fig. 5. Relationship between the measured pellet density and flame front velocity. The fitted curve is an exponential function.

4. Conclusions

Ball milling of Al and Ni powders causes extensive mechanical mixing and the formation of nanoscale lamellar microstructures with increasing milling time. With a ball to material weight ratio of 5.1:1 and a rotational speed of 300 rpm, 16–18 h of milling time produce easily ignitable powder mixtures with little intermetallic formation that exhibit self-propagating reactions, comparable to magnetron sputtered nanoscale multilayers. The reaction velocity increases with compacted pellet density due to enhanced thermal contact among the particles. Therefore, BM is shown to be an alternative viable method for the generation of micro and nanoscale heat sources for thermal manufacturing.

Acknowledgements

The authors would like to thank the European Commission for research funding of this project under Marie Curie Chair – UltraNanoMan (EXC-006680) and Marie Curie Excellence Team – NanoHeaters (EXT-0023899). In addition, the Department of Chemistry of University of Cyprus is acknowledged for providing access to XRD instrumentation.

References

[1] H. Jogdand, G. Gulsoy, T. Ando, J. Chen, C. Doumanidis, Z. Gu, C. Rebholz, P. Wong, Fabrication and Characterization of Nanoscale Heating Sources (Nanoheaters) for Nanomanufacturing, vol. 1, NSTI-Nanotech, 2008, pp. 280–283, ISBN: 978-1-4200-8503-7.
[2] I.E. Gunduz, K. Fadenberger, M. Kokonou, C. Rebholz, C.C. Doumanidis, Appl. Phys. Lett. 93 (2008) 134101.
[3] I.E. Gunduz, K. Fadenberger, M. Kokonou, C. Rebholz, C.C. Doumanidis, T. Ando, J. Appl. Phys. 105 (2009) 074903.
[4] K.J. Blobaum, D. Van Heerden, A.J. Gavens, T.P. Weihs, Acta Mater. 51 (2003) 3871–3884.
[5] A.J. Gavens, D.V. Heerden, A.B. Mann, M.E. Reiss, T.P. Weihs, J. Appl. Phys. 87 (3) (2000) 1255–1263.
[6] M. Atzmon, Solid State Powder Process. 90 (1990) 15560.
[7] L. Lu, M.O. Lai, S. Zhang, Mater. Des. 15 (2) (1994) 79–86.
[8] J. Meng, C. Jia, Q. He, Rare Met. 26 (4) (2007) 372–376.
[9] A. Hadjiafxenti, I.E. Gunduz, C. Tsotsos, T. Kyratsi, C. Doumanidis, C. Rebholz, Intermetallics, submitted for publication.
[10] F. Cardellini, G. Mazzone, M.V. Antisari, Acta Mater. 44 (4) (1996) 1511–1517.
[11] S.H. Fischer, M.C. Grubelich, 32nd AIAA/ASME/SAE/ASEE Joint Propulsion Conference, Lake Buena Vista, FL, July 1–3, 1996.
[12] J.J. Moore, H.J. Feng, Mater. Sci. 39 (1995) 275–316.
[13] H.C. Yi, J.J. Moore, J. Mater. Sci. 25 (1990) 1159–1168.
[14] P. Nash, M.F. Singleton, J.L. Murray, in: P. Nash (Ed.), Phase Diagrams of Binary Nickel Alloys, vol. 1, ASM International, Metals Park, Ohio, 1991.
[15] M. Atzmon, Phys. Rev. Lett. 64 (4) (1990) 487–491.
[16] J. Joardar, S.K. Pabi, B.S. Murty, J. Alloys Compd. 429 (2007) 204–210.

[17] H. Sieber, J.S. Park, J. Weissmuller, J.H. Perepezko, Acta Mater. 49 (2001) 1139–1151.
[18] M.H. Enayati, Z. Sadeghian, M. Salehi, A. Saisi, Mater. Sci. Eng. A 375–377 (2004) 809–811.
[19] F. Cardellini, G. Mazzone, A. Monotne, M.V. Antisari, Acta Metall. Mater. 42 (7) (1994) 2445–2451.
[20] C. Gras, N. Bernsten, B. Bernard, E. Gaffet, Intermetallics 10 (2002) 271–282.
[21] M.M. Moshksar, M. Mirzae, Intermetallics 12 (2004) 1361–1366.
[22] J. Li, F. Li, K. Hu, J. Mater. Process. Technol. 147 (2004) 236–240.
[23] S. Gennari, F. Maglia, U. Anselmi-Tamburini, G. Spinolo, J. Alloys Compd. 413 (2006) 232–238.
[24] L. Takacs, Prog. Mater. Sci. 47 (2002) 355–414.
[25] P. Zhu, J.C.M. Li, C.T. Liu, Mater. Sci. Eng. A 357 (2003) 248–257.
[26] J.J. Moore, H.J. Feng, Prog. Mater. Sci. 39 (1995) 243–273.
[27] J. Subrahmanyan, M. Vijayakumar, J. Mater. Sci. 27 (1992) 6249–6273.